sciendo

POLISH MARITIME RESEARCH 1 (105) 2020 Vol. 27; pp. 116-125
10.2478/pomr-2020-0012

STUDY ON HYDRODYNAMIC CONFIGURATION PARAMETERS OF VERTICAL-AXIS TIDAL TURBINE

Li Guangnian[1]
Qingren Chen[2]
Yue Liu[3]
Shanqiang Zhu[1]
Qun Yu[1]
[1] Ningbo University, China
[2] Wuhan Rules and Research Institute, China
[3] Liaoning Technical University, China

ABSTRACT

In this paper, a numerical code for predicting the hydrodynamic performance of vertical-axis tidal turbine array is developed. The effect of the tip speed ratio, solidity, and preset angle on the hydrodynamic performance are discussed using a series of calculations. The load principle of the rotor and the variation principle of the turbine power coefficient are studied. All these results can be considered as a reference for the design of vertical-axis tidal turbines.

Keywords: vertical-axis turbine, configuration parameters, structure strength, tidal energy, efficiency

INTRODUCTION

Compared with fossil energy, tidal energy is a pollution-free and renewable energy resource. All the countries in the world are competitively researching and developing the exploitation of tide energy technology [6, 18]. To exploit tidal energy, first that energy has to be converted into mechanical energy by a transducer, then the mechanical energy will be transformed into electric power by driving a generator. Thus, research on transducers is an important task for developing tidal energy. Traditional transducers can be divided into impeller-type and non-impeller-type. Tidal turbines are currently widely used as a kind of impeller-type transducer. Based on the turbine shaft direction and incoming flow direction, tidal turbines can also be divided into horizontal-axis turbines and vertical-axis turbines. If the turbine shaft is parallel to the incoming flow direction, it is called a horizontal-axis tidal turbine [8, 15]; if the turbine shaft is vertical to the incoming flow direction, it is a vertical-axis tidal turbine [3, 16, 17]. There are several vertical-axis turbines in use around the world including the following:

The AK-1000TM [1], SeaGen [4], Open Centre [2] in Ireland; Davis Hydro Turbine [12] and EnCurrent [9] in Canada; Gorlov [11] and OCGen [20] in the USA; Kobold [10] in Italy, are typical horizontal-axis tidal turbines. WanXiang , WanXiang 2 and HaiNeng 1 in China [14] are vertical-axis tidal turbines.

A typical vertical-axis turbine is shown in Fig. 1. Its blade can be assumed as a two-dimensional airfoil and is not limited by the direction of the current. The work speed ratio and the work noise of the vertical-axis tidal turbine are low, and the electrical power generating system can be installed above sea level. Therefore the vertical-axis tidal turbine has attracted extensive attention from researchers.

Fig. 1. Vertical-axis turbine

A whole vertical-axis tidal turbine consists of a main shaft which supports the turbine, vertical long blades and the connecting device between them. The work condition of the vertical-axis tidal turbine is not restricted by the incoming flow direction. That is, flow with the direction ranging from 0 to 360 degrees can drive the tidal turbine. There is no need to regulate the device for incident flow directions. Under interaction with the ocean current, the vertical-axis tidal turbine (lift-type) will start rotating. During one rotating cycle of the turbine, the blade approach stream velocity is the sum of the blade rotating speed and the current speed in the far field. Thus, the actual approach stream velocity of the blade changes with differences of its position angle, the lift and the drag. Because the rotation of the rotor is driven by a periodical lift force, the load on the turbine rotor is also periodic [5, 14].

As for a given blade airfoil, the main parameters that affect the energy conversion efficiency and structural strength of a vertical-axis tide turbine are the tip speed ratio, solidity, radius-chord length ratio and preset angle. In the following equations, Q is defined as the turbine torque, λ is the tip speed ratio and C_p stands for the energy utilisation coefficient. R, D and σ are the radius, diameter, and solidity of the turbine, respectively. C and b are the chord length and span of the blade. The number and deflection angle of the blades are written as N and φ. α, θ and ω represent the attack angle, turbine rotation angle, and rotating speed of the turbine. The speed of the incoming flow and the flow relative to the blade are defined as V and VR.

The positive flow is along its incoming direction and the corresponding positive direction of rotation is counterclockwise.

$$\lambda = \omega R/V \tag{1}$$

$$C_p = Q\omega/(0.5\rho V^3 Db) \tag{2}$$

$$\sigma = NC/\pi D \tag{3}$$

$$\tan\alpha = \frac{\cos(\theta+\varphi) - \lambda\sin\varphi}{\sin(\theta+\varphi) + \lambda\cos\varphi} \tag{4}$$

$$V_R = V\sqrt{1+\lambda^2+2\lambda\sin\theta} \tag{5}$$

$$Re = \rho V_R C/\mu \tag{6}$$

At present, there are several numerical methods for the hydrodynamic analysis of vertical-axis tidal turbines, including the stream-tube model method [19], the vortex model method [13], and the computational fluid dynamics (CFD) method [7]. With the stream-tube model method, based on the momentum theorem, it is hard to predict the flow field characteristics of turbines when the speed ratio increases to a certain extent. The classic vortex model uses a bound vortex filament to replace the rotor blade and changes its strength as a function of azimuthal position. But the model cannot match the Kutta condition, resulting in inaccurate calculation of the forces on the blades. The developed vortex model combined with a finite element analysis of the flow surrounding the blades improves the accuracy of the vortex model, but the computational cost is expensive. In recent years, the application of a CFD method to analyse the performance of turbines has become more popular, but too many factors can affect the results of CFD. So the results need to be verified by experimental tests. Further, the computational cost of CFD is huge, even though a small-scale model is usually used.

In this paper, an unsteady boundary element model is developed for hydrodynamic analysis of a vertical-axis tidal turbine. The performance of the tidal turbine is evaluated by changing three important parameters: the tip speed ratio, preset angle and solidity of the turbine. The influence rules of the three parameters on the hydrodynamic force, torque and power coefficient of the turbine are revealed by making a series of calculations. The research results can provide guidance for the design, optimisation and array layout of vertical-axis tidal turbines.

CALCULATING THEORY

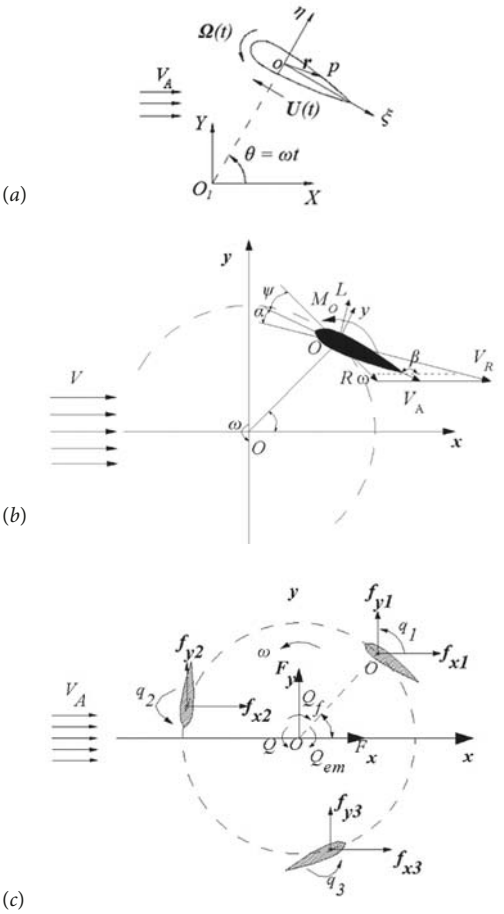

Fig. 2. Schematic diagram of blade motion

The schematic diagram of the blade motion is shown in Fig. 2. O is a reference point and U is the translational velocity of the blade. The rotational angular velocity is written as Ω. Uniform incoming flow is expressed as:

$$V_A = (V_{Ax}, V_{Ay}) \tag{7}$$

Defining $\Phi(p, t)$ as the velocity potential, it satisfies the Laplace equation in the fluid domain.

$$\nabla^2\Phi(p, t) = 0 \qquad (p \in \tau_e) \tag{8}$$

The non-penetration boundary condition on the blade surface is

$$\left.\frac{\partial\Phi}{\partial n}\right|_{S_b} = (U + \Omega \times r) \cdot n_b \tag{9}$$

where n_b is the normal of the blade surface, S_b; r is the vector from the origin, o, to any surface point in the coordinate system, $\zeta o\eta$. At infinity, $\Phi(p, t)$ satisfies the velocity potential for uniform incoming flow according to

$$\Phi(p, t) = xV_{Ax} + yV_{Ay} \qquad (p \to \infty) \tag{10}$$

If ϕ is the perturbation velocity potential, then Φ can be decomposed into two parts:

$$\Phi = xV_{Ax} + yV_{Ay} + \phi \tag{11}$$

Assuming a zero initial perturbation, ϕ should also satisfy the following equation and boundary conditions:

$$\nabla^2\phi(p, t) = 0 \qquad (p \in \tau_e) \tag{12}$$

$$\left.\frac{\partial\phi}{\partial n}\right|_{S_b} = (U - V_A + \Omega \times r) \cdot n_b \tag{13}$$

$$\nabla\phi \to 0 \qquad (p \to \infty) \tag{14}$$

$$\nabla\phi \to 0 \qquad (t = t_0) \tag{15}$$

where t_0 is the initial time.

The blade surface pressure coefficient is defined as:

$$C_p = \frac{p - p_\infty}{0.5\,\rho V_A^2} \tag{16}$$

So the load on the blade surface can be written as Eq. (17):

$$f = 0.5\rho V_A^2 \cdot \int_c C_p n dS \tag{17}$$

where S is the blade surface area.

The torque referred to the point O is:

$$q = 0.5\rho V_A^2 \cdot \int_{S_b} C_p (r \times n) dS \tag{18}$$

If all the forces acting on each single blade can get the force acting on the rotor, the resultant force F and the corresponding torque Q are calculated by:

$$F = \sum_{i=1}^{Z} f, \quad Q = \sum_{i=1}^{Z} f\, q_i \tag{19}$$

The coefficient of normal force acting on the blade is:

$$\overline{f} = \frac{f}{0.5\rho V^2\, Cb}$$

The coefficient of torque acting on the turbine rotor from a single blade:

$$C_q = \frac{q}{0.5\rho V^2\, Db \cdot R}$$

The coefficient of resultant forces acting on the rotor can be computed by

$$\overline{F} = \frac{F}{0.5\rho V^2\, Db}$$

The coefficient of average torque acting on the rotor is represented by

$$C_Q = \frac{Q}{0.5\rho V^2\, Db \cdot R}$$

RESULTS AND DISCUSSION

Many researchers have already made detailed studies on the hydrodynamic performance of the vertical-axis turbine, and Strickland's test is one of the most representative tests [15]. Using the numerical method proposed above, a simulation for the same model as Strickland's test is carried out under the same conditions, and the results compared with Strickland's test are shown in Fig. 3.

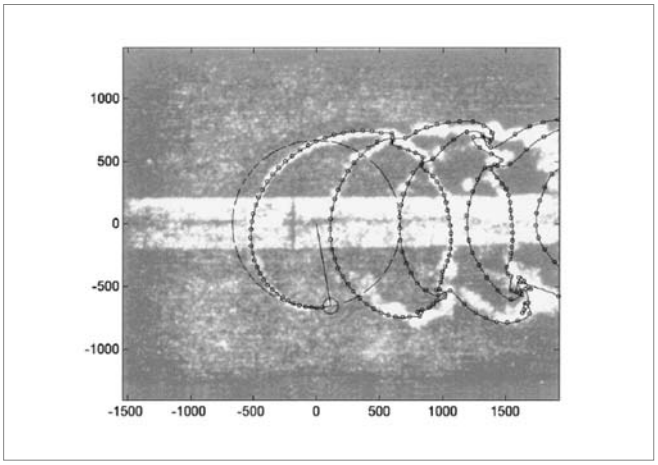

(a) Strickland's test results

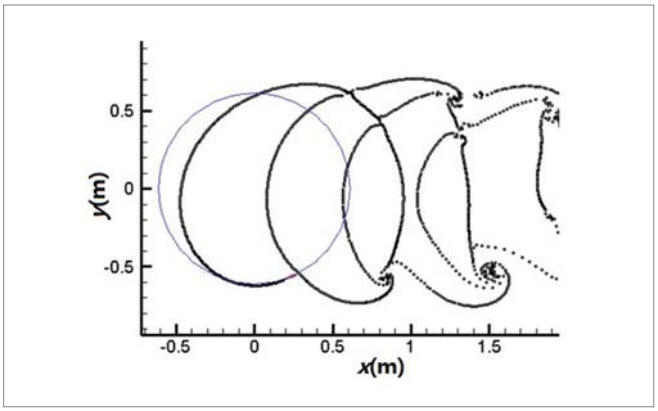

(b) Results predicted by this paper

Fig. 3. Simulation results compared with test results

Fig. 4 shows the calculation results of the present method compared with references for the same model under the same conditions. In these figures, the circles show the motion path of the turbine blade, the upper parts (blue) are the results from literature and the lower parts (red) are the present results. Through the comparison, we can see that the forecast of the turbine trailing vortex in this paper is in good agreement with the forecast results of the literature.

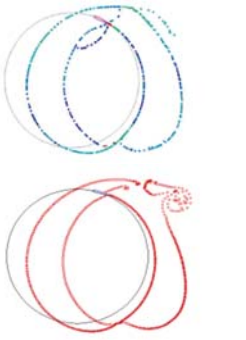

(A) θ = 780°

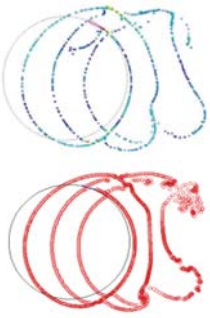

(B) θ = 1040°

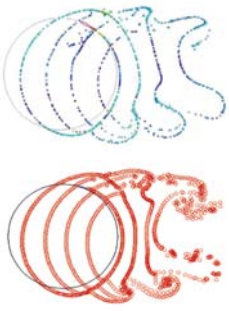

(C) θ = 1400°

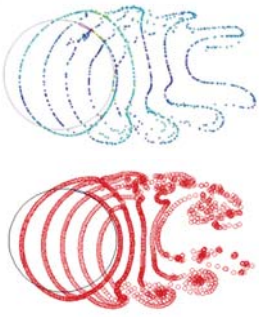

(D) θ = 1760°

Fig. 4. Calculation results compared with literature results

The hydrodynamic characteristics of a single vertical-axis tide turbine with fixed angle mainly includes the average and instantaneous torque of the rotor and energy conversion efficiency, the average and instantaneous load acting on the blade and the flow field characteristics, etc. The hydrodynamic characteristics of the turbine will be influenced by the installation position, deflection of the blade, tip speed ratio and solidity of the turbine. The effect of these parameters on the turbine efficiency and the load acting on the blade and rotor are analysed in detail in this paper.

ROTOR WAKE TRACK

Fig. 5 and Fig. 6 show the development process of the trailing vortex after the turbine blade. From the figures we can see that the blade passes through the fourth and the first quadrant successively when rotating, and crosses over the trailing vortex stream twice. The interference between the blades and trailing vortex is obvious when the blade rotates through the downstream area and crosses over the trailing vortex stream. At the same time, there is also interference between trailing vortices. As the wake vortices move down, the trailing vortex from different blades and the trailing vortex from the same blade at different time periods intertwine. After the blade passes through the fourth and first quadrant, two turn-up turbulent belts are generated in the trailing vortex stream. The turbulent belt in the first quadrant is obviously more disordered, mainly because the blade passes through the vortex downstream in the fourth quadrant and against the current in the first quadrant. The turbulent belt moves down with the trailing vortex, and moves gradually closer to the middle, and is finally broken down and dissipates when moving to a certain distance. The interference between the blade and trailing vortices is mainly concentrated in the downstream area. With the increase of the number of blades, the phenomenon of the blade passing through the trailing vortex becomes more frequent, and the interference between blades and vortices becomes more violent. In general, such intense interference is harmful to the turbine's hydrodynamic performance.

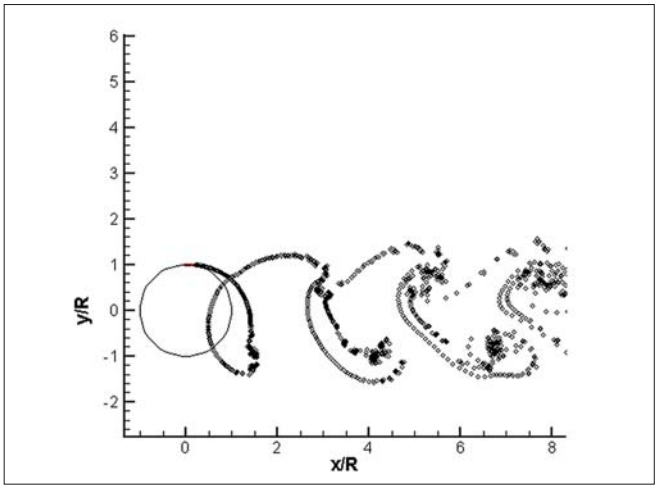

Fig. 5. Wake track with Z=1, λ=2

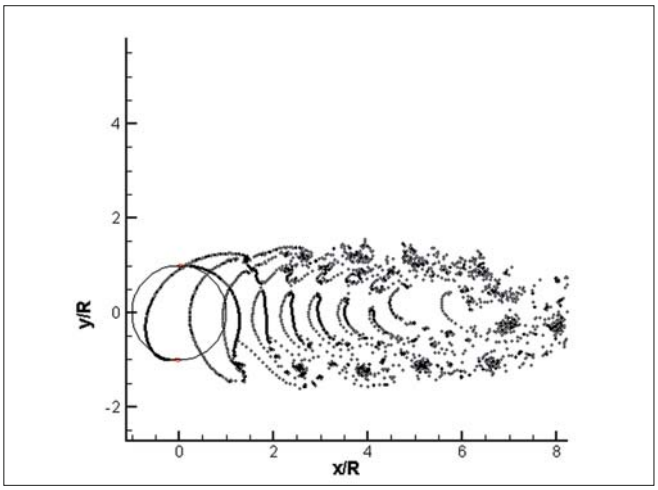

Fig. 6. Wake track with Z=2, λ=2

EFFECTS OF TIP SPEED RATIO ON HYDRODYNAMIC CHARACTERISTICS

In this paper, the effect of the tip speed ratio of a fixed-angle vertical-axis turbine on the transient load and average load on the blade and rotor is discussed. The diameter of the turbine model D = 2 m, blade number Z = 3, the blade airfoil is NACA0018, and chord C = 0.25 m.

By changing the tip speed ratio from λ = 1.2 to λ = 2.8, Fig. 7 shows the curves of the force coefficient varying with the angle of the blade position for different tip speed ratios, and the curves clearly show the blade force bearing status at different positions. In addition, during the rotation of the blades, the force on the blade increases along with the increase of its tip speed. The maximum value of all the blade force coefficients appears near to the position angle θ = 1170°. At this point the blade is in the upstream disc and the blade chord direction is perpendicular to the incoming flow; the blade resultant velocity is larger and so is the projected area along the direction of resultant velocity, therefore the force is larger. The minimum value appears in position angles θ = 1080° and θ = 1260°. In both of these positions, the blade chord line is parallel to the flow velocity; one position has the leading edge facing the flow, the other is toward the trailing edge. The position towards the flow area is small, resulting in a small force. Overall, the blade force values with θ changing from 1080° to 1260° were significantly higher than the force within the interval of θ changing from 1260° to 1440°. This is mainly because the interval where θ is changing from 1080° to 1260° is in the upstream disc and the interval where θ is changing from 1260° to 1440° is in the downstream disc. The small interference between the blade and vortex and between vortices results in a small force on the blade.

Fig. 8 shows the curves of force acting on the turbine rotor for several different tip speed ratios changing from λ = 1.6 to λ = 3.1, which vary with the position angle. The results show that the force acting on the turbine rotor is enhanced by the increasing tip speed ratio. The force acting on the rotor fluctuates periodically in a rotating period and will become more acute with the increasing tip speed ratio. Therefore, in the turbine design process, we should consider the periodical and maximum instantaneous load, besides the average force of the rotor.

Fig. 9 shows the variation of the moment coefficient on the same individual blades of the turbine with the change of position angle, at a tip speed ratio of λ = 1.6. Fig. 10 shows the torque coefficient of a single blade changing with the position angle for a number of different tip speed ratios. Fig. 11 shows the torque coefficient of the rotor changing with the position angle for a number of different tip speed ratios. When the torque coefficient of a single blade is positive, we define the corresponding range of the position angle as the output area. From Fig. 9 and Fig. 10, it can be seen that the output area is mainly in the upper disc, the peak appears near the position angle of the blade chord perpendicular to the flow velocity, and the moment coefficient is relatively small, even negative at some position angles. Since the torque coefficient of the total turbine rotor is the sum of a single blade, the torque coefficient in Fig. 11 shows the cyclical changes in one revolution of the turbine. From Fig. 7, Fig. 9 and Fig. 10, it can be seen that both the fluctuation of moment and the force acting on the blade in the downstream area of the turbine are always more violent than in the upstream region. It is also verified in the previous section that interference between the blade and trailing vortex and between vortices is more severe in the downstream area.

As can be seen from Fig. 10, both the mean coefficient and the peak coefficient of the turbine blade first increase and then decrease with the increment of the tip speed ratio. The turbine rotor torque coefficient is the same as the case in Fig. 11. Calculation of several tip speed ratios shows that the maximum torque coefficient appears at λ = 1.9. The analysis of this phenomenon is as follows. As is seen from Fig. 10 and Fig. 11, in most cases the tip speed ratio of the turbine blade torque values is negative in the downstream disc. Only when λ = 1.6 and λ = 1.9 is the torque coefficient positive, though still very small. Therefore, the torque of the blade in the upstream turbine disc contributes most of the total torque. When the blade rotates in the upper area of the disc, with the tip speed ratio becoming larger, the angle of attack becomes larger in the angle range of the best lift-to-drag ratio characteristic, and the moment coefficient increases. After the tip speed ratio exceeds a certain value, with the tip speed ratio increasing, the angle of attack range of the best lift-to-drag ratio decreases, which results in the torque coefficient decreasing.

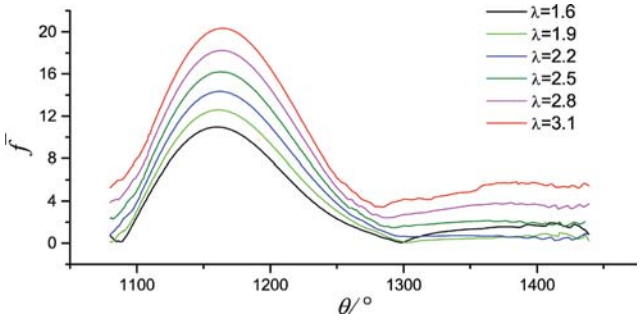

Fig. 7. Force coefficient of single blade, Z=3

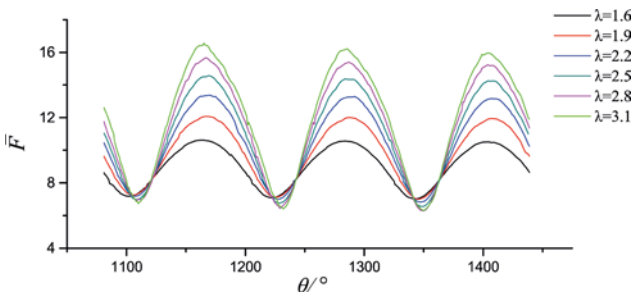

Fig. 8. Force coefficient of impeller, Z=3

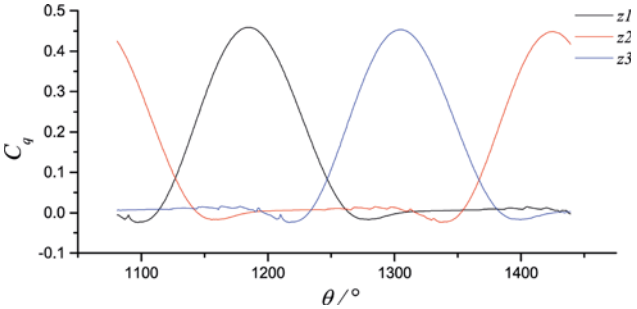

Fig. 9. Moment coefficient of three blades on the same turbine, Z=3, λ=1.6

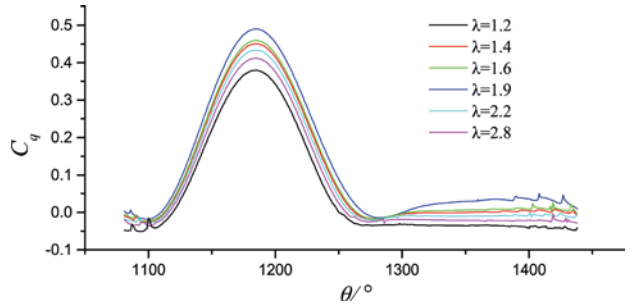

Fig. 10. Moment coefficient of single blade, Z=3

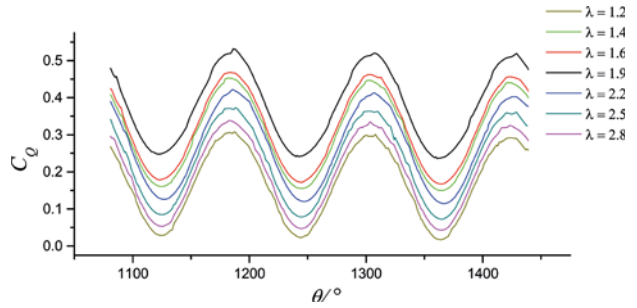

Fig. 11. Moment coefficient of impeller, Z=3

INFLUENCES OF BLADE PRESET ANGLE ON HYDRODYNAMIC CHARACTERISTICS

The blades have a preset angle when mounted on the rotor of the fixed angle vertical-axis turbine. The preset angle changes the distribution of the angle of attack during rotation of the turbine. The effects of the blade preset angle on the hydrodynamic performance of the turbine are discussed in detail below. The diameter of the turbine model D = 8.32 m, the blade chord C = 1 m, with the NACA0018 airfoil. We set the preset angle φ as: φ = 5°, φ = 3°, φ = 0°, φ = -3° and φ = -5°, and calculate two different tip speed ratios for each preset angle. The blade lies in the tangential direction of the locus circle of the turbine when φ = 0°. When the blade is outside the locus circle of the turbine (φ = 5°, φ = 3°), the absolute value of the angle of attack increases in the upstream disc and decreases in the downstream disc. The opposite happens when the blade is inside (φ = -3°, φ = -5°). The graphs in Fig. 12 show how the resultant force coefficient under different preset angle changes with the position angle. It can be seen from the figure that, compared to φ = 0°, in the upper reaches of the disc, the greater the outer partial preset angle is, the greater the blade resultant force coefficient is; the greater the inner partial preset angle is, the smaller the blade resultant force is. When there is an outer preset angle, the corresponding position angle of the force coefficient peak point advances. The greater the outer preset angle is, the further forward the peak point is. The opposite appears in the case of the blade's inner partial preset angle. In the downstream, the variation of force acting on the blade is more complicated. It is impossible to summarise the principle of the blade force from the calculated result. Because the magnitude of the force on the blade in the downstream is much smaller than in the upstream, the influence of the preset angle on the force of the blade in the downstream can be neglected.

The force acting on the turbine rotor for two tip speed ratios varies with the preset angle, which is shown in Fig. 13. It can be seen from the figure that the influence of the preset angle on the force acting on the turbine rotor is almost the same as that on the blade. Since the force on the rotor is the superposition of the force on the blade, which is shown in Fig. 13, the force during a rotation period fluctuates cyclically.

Fig. 14 shows that the torque coefficient of a single blade varies with the change of the blade preset angle. It can be seen from the figure that the blade moment coefficient increases with the increment of the preset angle when the blade rotates in the upper reaches of the disc, and changes oppositely when rotating in the downstream. The magnitude of the torque coefficient in the downstream disc is significantly smaller than in the upstream disc.

Fig. 15 shows that, for two tip speed ratios and five blade preset angles, the torque coefficient of the turbine rotor varies with the position angle. Overall, during one rotation of the turbine, both the mean and instantaneous values of the turbine rotor torque coefficient increase with the increment of the preset angle. It can be concluded that mounting the blades outside the locus circle of the turbine is beneficial to its energy utilisation efficiency, which is in agreement with other research findings in the literature.

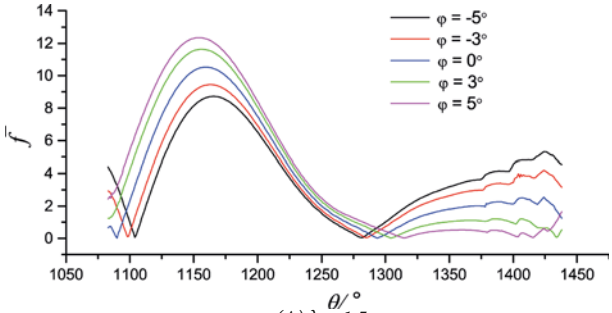

(A) λ = 1.5

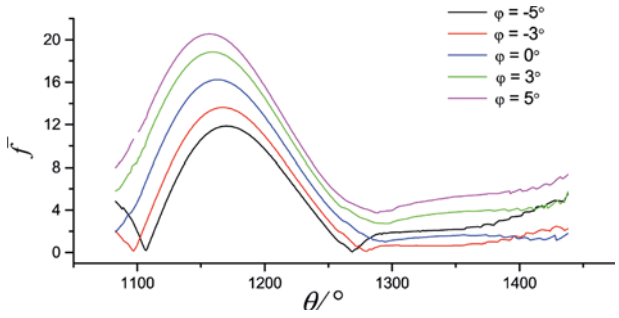

(B) λ = 2.5

Fig. 12. Single blade resultant force coefficient with different preset angles

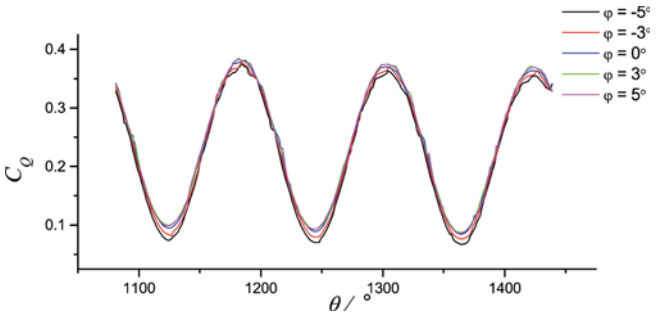

(B) λ = 2.5

Fig. 15. Turbine moment coefficient with different preset angles

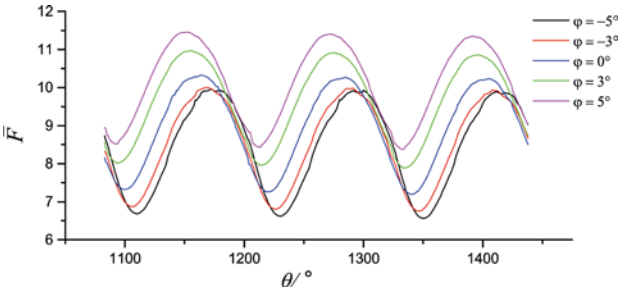

(A) λ = 1.5

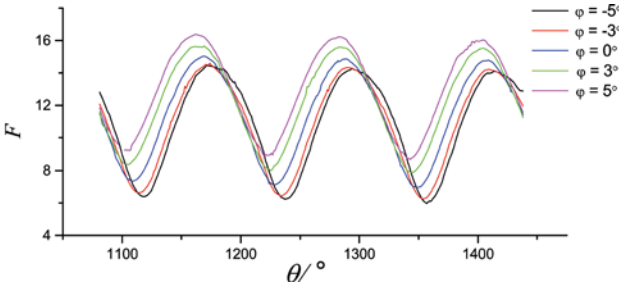

(B) λ = 2.5

Fig. 13. Turbine rotor force with different preset angles

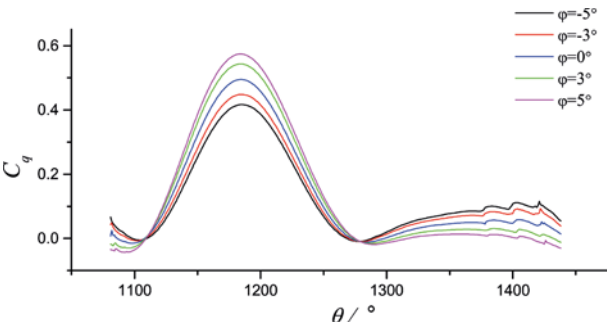

Fig. 14. Single blade moment coefficient with different preset angles, λ=1.5

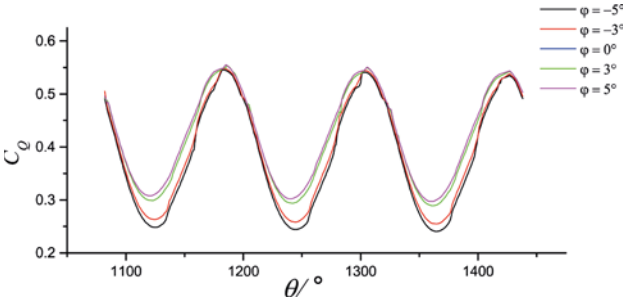

(A) λ = 1.5

EFFECTS OF BLADE SOLIDITY ON HYDRODYNAMIC CHARACTERISTICS OF THE TURBINE

The number of blades determines the interference intensity between the blades and trailing vortices, and between trailing vortices, which will be discussed below. The computing model airfoil blade is NACA0018, the blade chord C = 1 m, and the diameter of turbine D = 8.32 m. The hydrodynamic performance of the turbine with different blade numbers from Z = 1 to Z = 5 is discussed, and the corresponding solidity is σ_1 = 0.038, σ_2 = 0.077, σ_3 = 0.115, σ_4 = 0.153, and σ_5 = 0.191. The resultant coefficients of the single blade under different numbers of blades changing along the position angle in the case of the two tip speed ratios are shown in Fig. 16. It can be seen from the figure that with the increase of the blade number, the instantaneous peak force of the blade reduces, the difference of force on the blade in the upstream and downstream reduces, and the mean force on a single blade reduces. The blade force reduces mainly due to the interference from other blade impellers.

Fig. 17 shows how the rotor's resultant force coefficient of turbines with different blade numbers changes with the turbine position angle. It can be seen from the figure that, although the single blade force reduces, the force on the rotor still increases with increase of the blade number since the turbine rotor force is the superposition of the force on each blade. Meanwhile, with the increase of the blade number, during one rotation of the blades, the force on each blade is more stable. The instantaneous peak force on the turbine rotor is less than that of a turbine with fewer blades. From the viewpoint of either the blade force or the rotor force, the increase of the blade number is conducive to structural fatigue and vibration problems for the turbine.

Fig. 18 shows that the torque acting on a single blade of the turbine with different numbers of blades changes along the position angle. Fig. 19 shows that the moment acting on the rotor of the turbine with different numbers of blades changes along the position angle for the two tip speed ratios. It can be seen from Fig. 18 that with the increase of the blade number, the peak value of torque acting on a single blade reduces, and the peak corresponds to the same position angle. As can be seen from Fig. 19, with the increase of the blade number, the valley value of the turbine rotor torque coefficient increases, the peak decreases, the fluctuation of the torque

coefficient becomes smaller and the rotor torque output will be more stable. Assuming that there is no interference, the magnitude of torque acting on the rotor of the turbine with five blades should be 5 times that with one blade. From Fig. 19, with the increase of the blade number, the average torque on the rotor is not increased linearly. In the case of the tip speed ratio of $\lambda = 2.5$, the mean values of the torque coefficient of the rotor of the turbine with blade numbers from 1 to 5 are 0.222, 0.267, 0.236, 0.198, and 0.162. When $\lambda = 1.5$, the corresponding mean values are 0.192, 0.287, 0.304, 0.293, 0.277. This is sufficient to show that the interference between the blades is very complicated, and for the design of the turbine the selection of the blade number should be considered based on a variety of conditions.

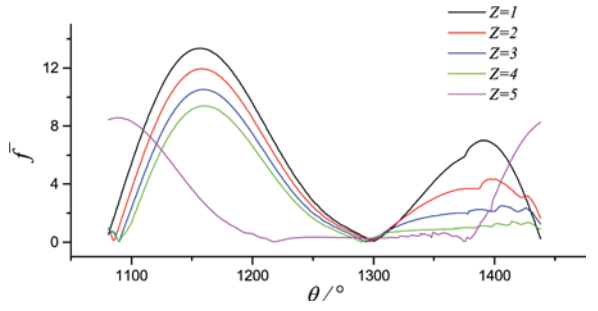

(A) $\lambda = 1.5$

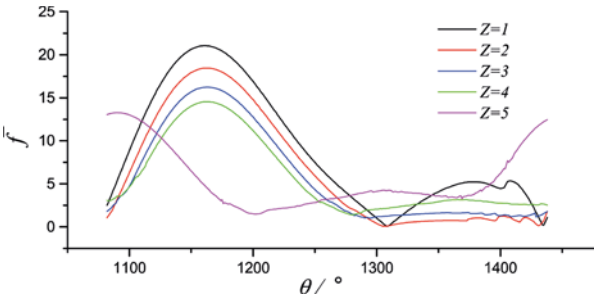

(B) λ=2.5

Fig. 16. The influence of different blade numbers on blade force

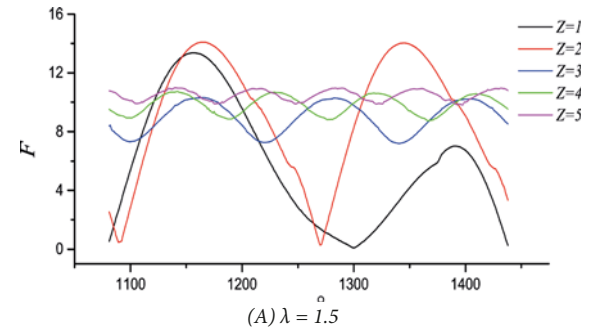

(A) $\lambda = 1.5$

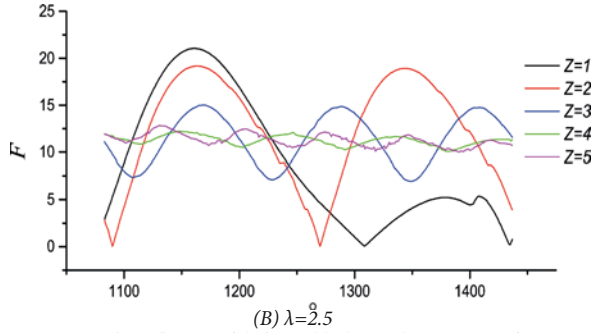

(B) λ=2.5

Fig. 17. The influence of different blade numbers on rotor force

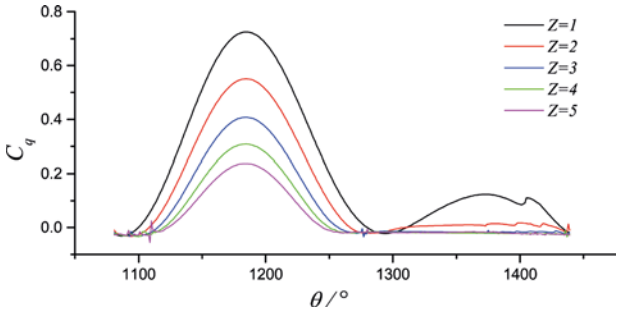

Fig. 18. The influence of different blade numbers on single blade moment

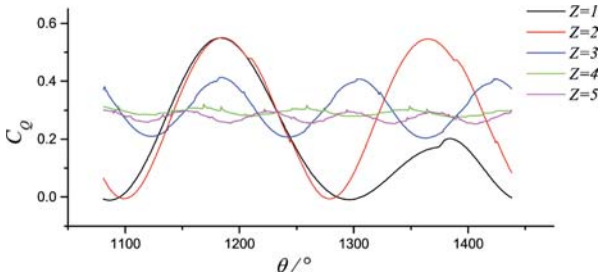

(A) $\lambda = 1.5$

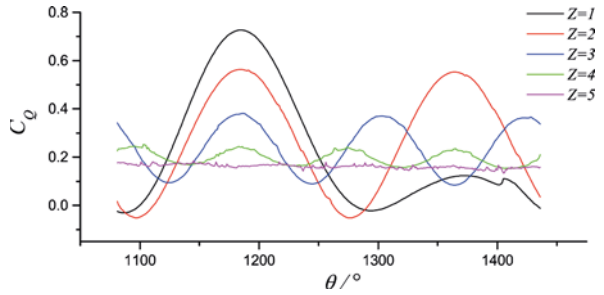

(B) λ=2.5

Fig. 19. The influence of different blade numbers on rotor moment

CONCLUSIONS

In this paper, the hydrodynamic characteristics of a vertical-axis tidal current turbine are analysed by numerical calculations. The results are consistent with those obtained by published tests. The influence of the structural parameters of the vertical- axis tidal turbine on the conversion efficiency and properties are analysed in detail. The results of the investigation of different configuration parameters of the vertical-axis turbine are presented as follows:

(1) Speed ratio: The loads in the flow field increase with the increase of the speed ratio. The change of the speed ratio means that the relative speed and angle of attack change at the same position angle. The speed ratio becomes larger and the angle of attack becomes smaller. The torque first increases to a maximum value and then decreases. The energy efficiency first becomes larger and then decreases. The design of the turbine should take full account of the working area of the water environment, in order to have the working speed ratio as close as possible to the optimal speed ratio range.

(2) The preset angle of the blade: When the leading edge of the blade is outside the locus circle of the turbine, it can

improve the energy utilisation efficiency of the turbine and decrease the load on the turbine and the blade, both of which are beneficial to the structure of the turbine. When the leading edge is in the locus circle, the condition is opposite to the former one. It is harmful to both the energy utilisation efficiency and the structure of the turbine.

(3) Solidity: Enlarging the solidity can increase the energy utilisation efficiency when the speed ratio is small. When the speed ratio becomes large, the opposite is true. The numerical results demonstrate that the larger the number of the blades, the higher the frequency is, and the smaller the amplitude of the fluctuation force and torque acting on the turbine rotor are. So it is better to use a smaller chord length radius ratio considering the load and energy output.

ACKNOWLEDGEMENTS

This study was funded by the China National Natural Science Foundation Program (grant number 51679216, 51579223) and Zhejiang Provincial Natural Science Foundation (grant number LY15E09007), and sponsored by the K. C. Wong Magna Fund in Ningbo University.

The authors declare that they have no conflict of interest.

REFERENCES

1. AK-1000 Tidal Turbine Project. https://www.power-technology.com/projects/aktidalturbine/.
2. Allsop S., Peyrard C., Thies P. R., et al. (2017): *Hydrodynamic analysis of a ducted, open centre tidal stream turbine using blade element momentum theory*. Ocean Engineering, 141, 531–542.
3. Jing F. M., Sheng Q. H., Zhang L. (2014): *Experimental research on tidal current vertical axis turbine with variable-pitch blades*. Ocean Engineering, 88, 228–241.
4. Joy R., Wood J. D., Sparling C. E., et al. (2018): *Empirical measures of harbor seal behavior and avoidance of an operational tidal turbine*. Marine Pollution Bulletin, 136, 92–106.
5. Li Z. C. (2011): *Numerical Simulation and Experimental Study on Hydrodynamic Characteristic of Vertical Axis Tidal Turbine*. Dissertation, Harbin Engineering University, pp. 33–38.
6. Lv X. G., Qiao F. L. (2008): *Advances in study on tidal current energy resource assessment methods*. Advances in Marine Science, 1, 98–108.
7. Marsh P., Ranmuthugala D., Penesis I. (2015): *Three-dimensional numerical simulations of straight-bladed vertical axis tidal turbines investigating power output, torque ripple and mounting forces*. Renewable Energy, 83, 67–77.
8. Myers L., Bahaj A. (2010): *Experimental analysis of the flow field around horizontal axis tidal turbines by use of scale mesh disk rotor simulators*. Ocean Engineering, 37, 218–227.
9. New Energy Corporation. https://www.newenergycorp.ca/encurrent-125-series.html.
10. http://www.seapowerscrl.com/ocean-and-river-system/kobold.
11. Ramos V., Iglesias G. (2013): P*erformance assessment of tidal stream turbines: A parametric approach*. Energy Conversion and Management, 69, 49–57.
12. Rourke F. O., Boyle F., Reynolds A. (2010): *Tidal energy update 2009*. Applied Energy, 87, 398–409.
13. Strikland J. H. (1975): *The Darrieus Turbine: A Performance Prediction Model Using Multiple Streamtubes*. Sandia Laboratory Report SAND 75-0431. Albuquerque, New Mexico: Sandia National Laboratories.
14. Wang L. B. (2006): *Theoretical and Experimental Study on Hydrodynamic Performance of Vertical-Axis Tidal Turbine*. Doctoral dissertation , Harbin Engineering University, pp. 46–48.
15. Wang S. Q., Sun K., Xu G., et al. (2017): *Hydrodynamic analysis of horizontal-axis tidal current turbine with rolling and surging coupled motions*. Renewable Energy, 102, 87–97.
16. Xie Y. H., Li G. N., Zhang Z. D. (2017): *Experimental analysis on arrangement rule of the twin-turbine systems with vertical axis tidal current turbines*. Acta Energiae Solaris Sinica, 38, 537–542.
17. Zanforlin S., Burchi F., Bitossi N. (2016): *Hydrodynamic interactions between three closely-spaced vertical axis tidal turbines.* Energy Procedia, 101, 520–527.
18. Zhang D., Li W., Lin Y. (2009): Wave energy in China: Current status and perspectives. Renewable Energy, 34, 2089-2092.
19. Zhang L., Wang L. B., Li F. L. (2004): *Streamtube models for performance prediction of vertical-axis variable-pitch turbine for tidal current energy conversion*. Journal of Harbin Engineering University, 25, 261–265.
20. Zhou Z. B., Benbouzid M., Charpentier J. F., et al. (2017): *Developments in large marine current turbine technologies – A review*. Renewable and Sustainable Energy Reviews, 71, 852–858.

CONTACT WITH THE AUTHORS

Li Guangnian
e-mail: liguangnian@nbu.edu.cn

Ningbo University
Fenghua Road, 315000 Ningbo
China

Qingren Chen
e-mail: cqr4891@126.com

Wuhan Rules and Research Institute
Liujiaoting Road, 430000 Wuhan
China

Yue Liu
e-mail: yue.liu@unipd.it

Liaoning Technical University
Yulong Road, 123000 Fuxin
China

Shanqiang Zhu
e-mail: zhushanqiang@nbu.edu.cn

Ningbo University
Fenghua Road, 315000 Ningbo
China

Qun Yu
e-mail: yuqun@nbu.edu.cn

Ningbo University
Fenghua Road, 818 Ningbo
China